J Wood Sci (2009) 55:91–99
DOI 10.1007/s10086-008-1009-x

ORIGINAL ARTICLE

Wook Kang · Woo Yang Chung

Liquid water diffusivity of wood from the capillary pressure–moisture relation

Received: August 18, 2008 / Accepted: November 25, 2008 / Published online: February 3, 2009

Abstract This study focuses on liquid water transport in wood above the fiber saturation point in the nonhygroscopic region. The liquid water transport of hygroscopic porous materials including wood is usually described by Darcy's law. It requires knowledge of capillarity and intrinsic and relative permeabilities. In this study, the capillary pressure–water relation and relative permeability were investigated using experimental data for wood available in the literature. The performance of three models (Brooks-Corey model, van Genuchten model, and Durner's bimodal pore-size distribution model) was investigated for the capillary pressure–water relation. These models have advantages in that each shape parameter has qualitative physical meaning for the pore-size distribution. Most species had unimodal pore distributions except for aspen, which had a bimodal pore distribution. The van Genuchten model represented the capillary pressure–water relation better than the Brooks-Corey model. Durner's bimodal model was found to be the most appropriate for the capillary pressure–moisture relation of aspen. The relative permeability was calculated by using Mualem's model, which was compared with the value from the Couture model. From the results, the liquid water diffusivity divided by intrinsic permeability of wood was estimated. This approach may be promising for adopting the liquid water diffusivity for the numerical simulation of drying and sorption, although there might be considerable variation within and between trees.

Key words Liquid water transport · Capillary pressure · Permeability · Wood · Nonlinear fitting

W. Kang (✉) · W.Y. Chung
Department of Wood Science and Engineering, Division of Forest Resources and Landscape Architecture, Chonnam National University, Gwangju 500-757, Republic of Korea
Tel. +82-62-530-0294; Fax +82-62-530-2099
e-mail: kawook53@msn.com

Introduction

Several models for simulating the transport of heat and moisture in wood have been developed recently. Most models have been validated by experiment. Among them, sophisticated and widely accepted models that have three systems of governing equations are for the behavior of wood drying processes.[1–3]

Above the fiber saturation point (FSP), wood is nonhygroscopic, and most models assume that liquid water transport follows Darcy's law. Bound water movement in the hygroscopic range follows Fick's law. For the simulation of liquid water transport in wood, therefore, three material indices such as intrinsic and relative permeability as well as the capillary pressure–moisture relation (CMR) or the capillary pressure–saturation relation (CSR) are required. For the combined bound water movement, three indices such as the sorption isotherm, bound water diffusivity, and water vapor diffusivity are necessary. Therefore, the simulation of moisture transport in the whole moisture range requires six material indices that should be measured in independent experiments.

The successful application of heat and moisture transport models depends on the reliability of information on the material parameters necessary for the governing equations. However, most models contain at least one adjustable parameter, which must be determined by independent experiment, and so are not completely predictive. In some cases, some properties are adopted arbitrarily from other studies without investigating the whether the inclusion of such data is appropriate. To review and develop heat and moisture transport models, it should be noted that sophisticated models do not necessarily provide better prediction without minimizing uncertainties in input parameters.

Heat and moisture transport coefficients are dependent on grain orientation, hysteresis, and the local values of moisture content and temperature, as well as physicochemical properties of wood species. Furthermore, the material properties of wood are highly variable even within one tree. Thus, the information on heat and moisture transport

coefficients is very limited because considerable experimentation is required to ascertain them for all possible conditions. Indeed, the measurement of coefficients at a given temperature and moisture content is a very time-consuming process.[4] This is a major limitation for practical application of the models. For liquid water transport in wood, above all, it is difficult to find studies that deal with all three properties mentioned above.

The purpose of this study was to investigate an appropriate model for the CSR and the relative permeability of wood using experimental data available in the literature and to estimate the liquid water diffusivity as a function of saturation.

Theory

The hygroscopic porous material consists of the solid matrix, dry air, and moisture. Moisture is the sum of bound water, water vapor, and liquid water. In wood science, liquid water is called free water. Moisture transport models for isothermal conditions can be divided into three types according to the driving potential (Table 1). Using chain rules, any assumed driving potential can be changed to the equivalent potential of moisture gradient.

In this study, it is assumed that

1. wood density does not change with moisture content (neglecting dimensional change)
2. gas pressure in wood is constant (neglecting bulk flow of fluid)
3. temperature is constant (neglecting moisture transport due to temperature gradient)

Model 1

Darcy's law has been widely used for liquid water transport while Fick's law has been used for bound water and water vapor transport. Assuming the driving potentials of capillary pressure and moisture gradient, the multiphase moisture transport equation for wood can be expressed as Eq. 1.

$$\frac{\partial m}{\partial t} = \nabla \cdot \left[-\frac{\rho_w}{\rho_0} \frac{k_{rw} K_w}{\nu_w} \nabla P_c + (D_v + D_B) \nabla m \right] \quad (1)$$

where m is moisture content based on the moisture fraction per unit dry wood, ρ_0 is the oven-dry wood density, ρ_w is the liquid water density, k_{rw} is the relative water permeability, K_w is intrinsic water permeability, ν_w is dynamic viscosity of liquid water, P_c is capillary pressure, D_v is diffusivity of water vapor, D_B is diffusivity of bound water.

Bound water and water vapor transport in wood are interdependent and can be combined, which results in combined bound water and water vapor diffusivity.[5,6] Equation 1 can be expressed in terms of a single driving potential of moisture gradient by using chain rules if the dependence of capillary pressure on saturation or moisture content can be identified.

$$\frac{\partial m}{\partial t} = \nabla \cdot \left[\left(D_w + \overline{D_v + D_B} \right) \nabla m \right] \quad (2)$$

where D_w is liquid water diffusivity and can be expressed as

$$D_w = -\frac{\rho_w}{\rho_0} \frac{k_{rw} K_w}{\mu_w} \frac{\partial P_c}{\partial S} \frac{\partial S}{\partial m} \quad (3)$$

The relationship between saturation and moisture content should be given for converting the CSR into CMR. When the moisture content is above the FSP, the water saturation (S) can be calculated by

$$S = \frac{m - m_{FSP}}{m_{max} - m_{FSP}} \quad \forall m > m_{FSP} \quad (4)$$

where m_{FSP} is the FSP of wood, which is usually assumed to be 0.3.

For hygroscopic materials such as wood, it should be noted that by adopting an irreducible saturation concept ($m_{irr} > m_{FSP}$), the set of equations may produce a mathematical singularity as Couture et al.[3] indicated.

The water dynamic viscosity is calculated by

$$\nu_w = \rho_w \exp\left(-19.143 + \frac{1540}{T + 273.15} \right) \quad (5)$$

Therefore, three material parameters ($\partial P_c/\partial m$, k_{rw}, K_w) should be determined for the prediction of liquid water diffusivity under isothermal conditions.

Model 2

In the case of using water potential as the driving potential,

$$\frac{\partial m}{\partial t} = \nabla \cdot \left(\frac{K}{\rho_0} \nabla \psi \right) \quad (6)$$

Table 1. Material properties to be measured and estimated by models

Model	Driving potential	Material properties			References
		Nonhygroscopic region	Hygroscopic region	Estimation by inverse method	
1	Capillary pressure, moisture gradient	CSR, intrinsic and relative permeability	Sorption isotherm, bound water and water vapor diffusivity	–	1,2
2	Water potential	CSR, sorption isotherm		Effective moisture conductivity	9,10,18
3	Moisture gradient	–		Effective moisture diffusivity	25–27

CSR, Capillary pressure–saturation relation

where ψ is the water potential and K is the effective moisture conductivity.

The water potential is the energy that is needed to transport unit moisture, which is the sum of the matric and osmotic potential. It is usually applied in soil science. The relationship between the capillary pressure and the water potential is

$$P_c = \frac{2\sigma\cos\theta}{r} = -\rho_w\psi \tag{7}$$

where σ is the surface tension of water, r is the radius of curvature of the air–water interface into the capillaries, and θ is the contact angle between the water and the surface of the capillary.

Similarly to Eq. 3, Eq. 6 can be expressed as Eq. 8 from the relation between moisture content and water potential or capillary pressure to be determined

$$\frac{\partial m}{\partial t} = \nabla\cdot\left(\frac{K}{\rho_0}\frac{\partial\psi}{\partial m}\nabla m\right) = \nabla\cdot\left(-\frac{K}{\rho_0\rho_w}\frac{\partial P_c}{\partial m}\nabla m\right) \tag{8}$$

Comparing Eq. 8 with Eq. 3, the effective moisture conductivity has the physical meaning involving terms of intrinsic and relative permeability.

$$K = \rho_w^2\frac{k_{rw}K_w}{\mu_w} \tag{9}$$

K cannot be determined directly and so Cloutier and Fortin[7] determined it using the instantaneous moisture profile method in non-steady-state conditions during drying.

Model 3

In building physics, a nonlinear diffusion equation is often used for simplicity:

$$\frac{\partial m}{\partial t} = \nabla\cdot(D\nabla m) \tag{10}$$

where D is the effective moisture diffusivity.

D involves the combined effects of liquid water, water vapor, and bound water diffusivities, and is often expressed as an exponential function. It is usually obtained by the Boltzmann transformation method during sorption and by the moisture gradient method during drying.[8] The Boltzmann transformation method cannot be used for drying because it requires the moisture content at one end to be maintained at the initial moisture content.

Recently, Kang et al.[5,6] studied bound water and water vapor transport in the hygroscopic region. The present study focuses mainly on liquid water transport above the FSP. From Eqs. 2, 8, and 10, the effective liquid water diffusivity should be the same in terms of moisture content regardless of which driving potential is used.

$$D_w = -\frac{\rho_w}{\rho_0}\frac{k_{rw}K_w}{\mu_w}\frac{\partial P_c}{\partial S}\frac{\partial S}{\partial m} = -\frac{K}{\rho_0\rho_w}\frac{\partial P_c}{\partial m} \tag{11}$$

It should be noted that $\partial P_c/\partial m$ is negative because capillary pressure increases with decreasing moisture content. The CSR in the hygroscopic range (below FSP) may be calculated by the Kelvin equation using the sorption isotherm.[9]

Results and discussion

The CSR and relative permeability, apart from intrinsic permeability, were investigated among three material indices for the simulation of liquid water transport.

Capillary pressure–saturation relation

The CSR that is usually referred to as the water retention curve in soil science cannot be determined theoretically. Measurements of the CSR of wood are very scarce when compared with studies of other building materials such as concrete and soil. Most CSRs of wood that have been measured are for desorption. Very rarely is the CSR curve measured during absorption and the only example may be that of western hemlock by Fortin.[10]

The CSR is determined by direct methods (centrifugal method, pressure plate and pressure membrane method) or indirect methods (mercury intrusion porosimetry, image analysis).[8,11]

Table 2 shows empirical equations for the CSR of wood during desorption or drying. Spolek and Plumb[4] used models similar to those suggested by Brooks and Corey[12] for south-

Table 2. Empirical equations for capillary pressure–saturation relation of wood

Equation	Constants	Species	Reference
$P_c(S) = a_1 S^{-a_2}$	$a_1 = 8.4\times10^4$, $a_2 = 0.63$	Southern pine	4
$P_c(S,T) = 101325[a_1 S\exp(-a_2 S) + a_3(1-S)S^{-a_4}]\left(1-2.79\cdot10^{-3}(T-273)\right)$	Heartwood $a_1 = 12.12$, $a_2 = 5.939$, $a_3 = 0.046$, $a_4 = 3.7$ Sapwood $a_1 = 1.937$, $a_2 = 3.785$, $a_3 = 0.093$, $a_4 = 1.4$	Pine	13
$P_c(S,T,\rho) = \sigma(T)\left[\frac{a_1}{S+a_2} - \frac{a_3+a_4\rho_0}{a_5-S} + a_6\rho_0(1-S) + a_7 + a_8\rho_0 - \frac{a_9}{1+a_{10}}\right]$	$a_1 = 3150$, $a_2 = 1.0\times10^{-4}$, $a_3 = 1047$, $a_4 = 3.368$, $a_5 = 1.02$, $a_6 = 149.8$, $a_7 = 52\,350$, $a_8 = 168.4$, $a_9 = 3150$, $a_{10} = 1.0\times10^{-4}$	Softwood	14
$P_c(S,T) = \sigma(T)\sqrt{\frac{\phi}{K_w}}J(S)$ $J(S) = \frac{a_1}{S-a_2} + \frac{a_3}{S+a_4} - a_5 S + a_6$	$a_1 = 9.547\times10^{-3}$, $a_2 = 1.028$, $a_3 = 2.0023\times10^{-2}$, $a_4 = 0.0$, $a_5 = 1.2\times10^{-5}$, $a_6 = 4.415\times10^{-3}$	Bed of glass spheres	15

$\sigma(T) = (77.5 - 0.185(T - 273.15))\times10^{-3}$

ern pine in the tangential direction using the centrifuge method. Bonneau and Puiggali[13] deduced the capillary pressure curves from data obtained by mercury intrusion porosimetry. Using image analysis, Perre and Turner[14] estimated them as a function of local density for softwood. In addition, Perre and Moyne[15] adopted the Leverett function to fit experimental data for a bed of glass spheres that is frequently used in soil science.

Capillary pressure is strongly nonlinear with moisture content although it was plotted as the logarithm function, as shown in Fig. 1a. Power, exponential, or rational functions were used to fit the experimental data for the CSR (Table 2). Each expression for nonlinear curve fitting is different among the models, and is not generalized. However, a power function type of the CSR based on Spolek and Plumb[4] is often adopted for softwood drying without much correction of parameter values.[16,17]

Unfortunately, the experimental data are not available directly and the CSR have been digitized from graphs that can be found in the literature. Figure 1b shows the CSR measured by the pressure plate method[9,10,18] and Fig. 1c,d shows the CSR measured by the centrifugal method.[19] As expected, capillary pressure changes by the pressure plate method can be obtained over a wider range of saturation. However, most of the experimental data measured by the centrifugal method are in a limited range of saturation from 0.2 to 0.6.

Aspen distinctly represents the characteristic bimodal CSR curves but other species represent typical unimodal curves. The measured capillary pressure ranged from 10^3 to 10^7 Pa depending on saturation. Western hemlock represents high hysteresis and the capillary pressure was two orders of magnitude less than desorption or drying, as shown in Fig. 1b. At the same saturation, the capillary pressure of heartwood is expected to be higher than that of sapwood due to higher pit aspiration rate. On the contrary, however, the capillary pressures for the heartwood of American elm and cottonwood were less than for sapwood,

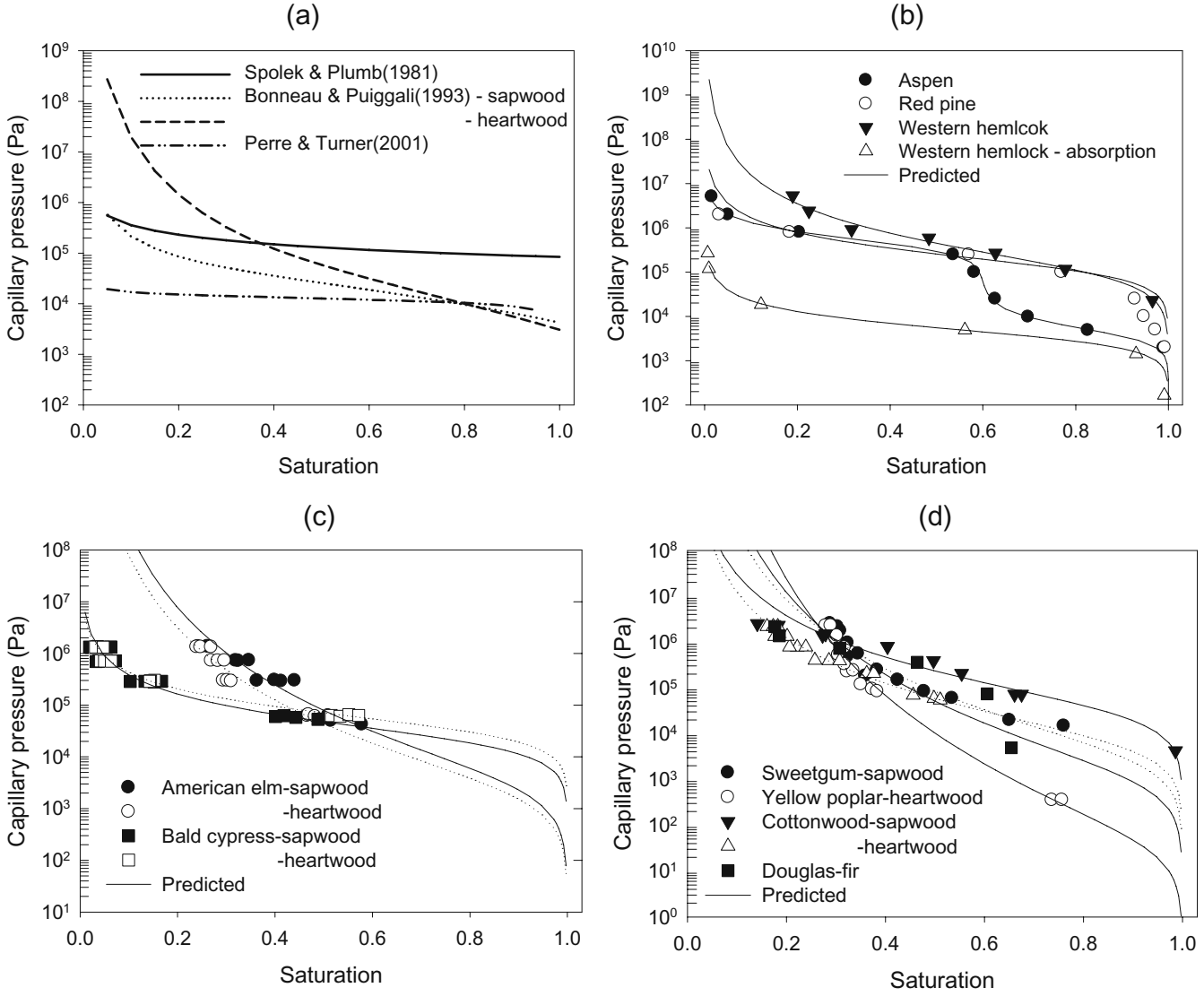

Fig. 1a–d. Capillary pressure versus saturation of wood at room temperature and fitted curves of van Genuchten and Durner models. **a** Empirical equations, **b** pressure plate method, **c** and **d** centrifugal method. *Solid line*, heartwood; *dotted line*, sapwood

the cause of which is unclear. It is interesting that the variation of the CSR is not high compared with intrinsic permeability. The difference in intrinsic permeability is several orders of magnitude even within the same species.[20]

Inverse estimation of parameters by CSR models

The CSR curves can be fitted to an exponential function with polynomials. Table 3 shows the best fitted parameters for the experimental data (Fig. 1b–d), in which saturation was converted to moisture content using Eq. 4. Adopting the exponential function, however, there are some limitations because no information can be obtained for the pore-size distribution and at least three parameters are needed for nonlinear fitting.

Table 4 shows unimodal and multimodal models for the CSR. Brooks and Corey (BC)[12] and van Genuchten (VG)[21] models represent unimodal pore-size distribution models having two undetermined parameters. The Durner (DN)[22] model is often used as a multimodal pore-size distribution model, in which the CSR subcurves representing the pore-size subsystems can be linearly superimposed by the VG model.

For the BC model, P_{cb} is the air entry capillary pressure value and λ characterizes the pore-size distribution. Its value approaches infinity for a medium with uniform pore size, whereas it approaches zero for a medium with a wide range of pore sizes. For the VG model, mn or $n–q$ corresponds to λ if the product mn remains constant, and α is related to the inverse of the air entry value, but strict definition is not clear.

Table 5 shows shape parameters for models with the best nonlinear curves fitted for the CSRs. The VG models gave better fitting results than the BC models in most cases. For aspen with a bimodal pore structure, shape parameters of the DN bimodal model are given in Table 6. When the CSR curve can be fitted with unimodal models, there may be no need to use DN multimodal models. However, the Durner bimodal model may give better fitting results in less fitted cases such as Douglas fir. Using the best fitted shape parameters, the fitted CSR curves are shown in Fig. 1b–d.

Table 3. Exponential equation for capillary pressure–saturation relation, $P_c = \exp(a_1 + a_2m + a_3m^2 + a_4m^3 + a_5m^4)$

Method	Species	a_1	a_2	a_3	a_4	a_5	R^2
Pressure plate method	Aspen	24.492	–50.443	86.929	–64.735	16.224	0.979
	Red pine	16.348	–0.3909	–17.761	21.228	–7.0789	0.990
	Western hemlock						
	–	25.608	–25.901	18.418	–4.748	–	0.982
	Absorption	20.097	–34.215	32.214	–8.9183	–	0.983
Centrifugal method	American elm						
	Sapwood	17.065	–2.219	–3.229	–	–	0.955
	Heartwood	35.385	–46.594	22.267	–	–	0.943
	Baldcypress						
	Sapwood	17.296	–11.672	5.338	–	–	0.954
	Heartwood	19.559	–20.837	12.596	–	–	0.979
	Cottonwood						
	Sapwood	15.463	–1.427	–0.539	–	–	0.995
	Heartwood	16.862	–6.161	1.232	–	–	0.982
	Sweetgum						
	Sapwood	22.749	–19.869	7.658	–	–	0.948
	Yellow poplar						
	Heartwood	29.344	–30.596	9.956	–	–	0.984
	Douglas fir	12.998	6.223	–7.648			0.928

Table 4. Unimodal and multimodal models for capillary pressure–saturation relation, and its relative permeability by the Mualem model

Model	Capillary pressure	Relative permeability
Brooks and Corey[12]	$S = \left(\frac{P_c}{P_{cb}}\right)^{-\lambda}$	$k_{rw} = S^{p+r+q/\lambda}$
	$(P_c > P_{cb})$	
Mualem[28]	$S = \left[1+(\alpha P_c)^n\right]^{-m}$	$k_{rw} = S^p\left[1-\left(1-S^{1/m}\right)^m\right]^r$
	$(\alpha > 0, n \geq 1, m = 1 - q/n)$	
van Genuchten[21]	$S = \sum_{i=1}^{k} w_i S_i$	$k_{rw} = S^p\left(\frac{\sum_{i=1}^{k} w_i\alpha_i\left[1-(1-S_i^{1/m_i})^{m_i}\right]}{\sum_{i=1}^{k} w_i\alpha_i}\right)^r$
	$S_i = \left[1+(\alpha_i P_c)^{n_i}\right]^{-m_i}$	
	$\alpha_i > 0, n_i \geq 1, m_i = 1 - q/n$	
	$0 < w_i < 1, \sum w_i = 1$	

Table 5. Shape parameters for capillary pressure–water relation by the Brooks and Corey and van Genuchten models

Species	Brooks and Corey			van Genuchten		
	P_{cb}	λ	R^2	α	n	R^2
Softwood						
Red pine	2000	0.1531	0.6978	7.169×10^{-6}	1.921	0.9848
Western hemlock						
–	23000	0.2648	0.9176	9.145×10^{-6}	1.464	0.9896
Absorption	164	0.2397	0.7765	2.669×10^{-4}	2.275	0.9997
Baldcypress						
Sapwood	20490	0.7873	0.9842	4.212×10^{-5}	1.826	0.9844
Heartwood	31496	0.8832	0.9934	2.510×10^{-5}	1.969	0.9945
Douglas fir	626	0.1612	0.7461	1.200×10^{-3}	1.168	0.7518
Hardwood						
Aspen	1950	0.2154	0.8676	1.740×10^{-4}	1.282	0.8854
American elm						
Sapwood	2421	0.1993	0.9293	3.906×10^{-4}	1.201	0.9300
Heartwood	1773	0.2157	0.9493	5.544×10^{-4}	1.216	0.9488
Cottonwood						
Sapwood	4250	0.1979	0.8849	3.186×10^{-5}	1.336	0.9615
Heartwood	5792	0.2998	0.9790	1.604×10^{-4}	1.304	0.9796
Sweetgum						
Sapwood	2517	0.1983	0.9461	3.756×10^{-4}	1.200	0.9414
Yellow poplar						
Heartwood	28	0.1177	0.9882	3.380×10^{-2}	1.118	0.9879

Table 6. Shape parameters for capillary pressure–water relation by Durner bimodal model

Species	w_1	α_1	n_1	α_2	n_2	R^2
Aspen	0.5966	2.192×10^{-6}	2.669	2.274×10^{-4}	2.687	0.9994
Douglas fir	0.6273	2.998×10^{-6}	1.755	3.739×10^{-4}	5.208	0.9927

The shape parameter λ may change from 0.19 to 11.67 depending on soils[20] but it ranges from 0.1177 to 0.8832 in cases of the wood investigated in this study. According to the BC model, yellow poplar might have a wider pore-size distribution than baldcypress. Comparing the λ of the BC model and n of the VG model, λ is close to n–1 in most wood species. In the case of absorption of western hemlock, however, there is a large difference in q of desorption because q is close to 2 for absorption but 1 for desorption.

Relative permeability

For the relative permeability of wood, an excellent review is provided by Couture et al.[3] Due to difficulties in measuring relative permeability, many methods for estimating it as a function of saturation or capillary pressure have been developed in soil science and petroleum engineering. It can be divided into two groups: those based on the CSR[12,21,22] and those expressed empirically in a power function of saturation. According to Couture et al.,[3] the accuracy of the relative permeability determined experimentally remains unclear for most materials and arbitrary power functions are often used in heat and moisture transport modeling. Especially in the case of wood, the experimental data are extremely limited except for Tesoro et al.[23] The estimation of relative permeability is still open to discussion because there is little experimental evidence.

First, the arbitrary power function is frequently used for wood drying

$$k_{rw} = S^n \quad (n > 1, 0 < S < 1) \tag{12}$$

where n is different in the structural direction due to the anisotropy of wood ($n = 3$ in transverse direction and $n = 8$ in the fiber direction).[2]

Second, the relative permeability can be estimated using the general expression of the Mualem model if the CSR is known in advance.[24]

$$k_{rw} = S^p \left(\frac{\int_0^S P_c(S)^{-q} dS}{\int_0^1 P_c(S)^{-q} dS} \right)^r \tag{13}$$

in which the parameters p (≤ 0), q (>0), and r (>1) determine the shape of the relative permeability function. p is a lumped parameter that accounts for pore connectivity and tortuosity. Therefore, using the generalized Mualem model (Eq. 13), the relative permeability of the BC, VG, and DN models can be obtained as shown in Table 4. In this study, we adopt the Mualem model ($p = 0.5$, $q = 1.0$, $r = 2$).

Third, the partial derivative of capillary pressure with respect to saturation is decreasing without bound ($-\infty$) because capillary pressure increases indefinitely as satura-

tion tends toward zero. This results in indeterminate value of liquid velocity. Therefore, the relative permeability of the liquid phase was given by using the following form:[3]

$$k_{rw} = S^p \left(\min_{S<s<1} \left| \frac{\partial P_c}{\partial S} \right| \Big/ \left| \frac{\partial P_c}{\partial S} \right| \right) \quad \text{with} \quad 0 < p \le 1 \tag{14}$$

Comparing the predicted drying results with the experimental data for pine, Couture et al.[3] used the same capillary pressure–water relation given by Bonneau and Puiggali[13] and obtained the best agreement by using $p = 0.3$.

For the anisotropic materials such as wood, the relative permeability may not be dependent on the structural direction because the CSR is not dependent on the structural direction of test samples.[19] Depending on the structural direction of wood, therefore, the main difference in liquid water diffusivity might be due to the intrinsic permeability.

Using the VG model for the CSR, the relative permeability by Mualem and Couture models can be calculated as shown in Fig. 2. The nonlinearity of the relative permeability with saturation increases as n decreases and r increases. Compared with the Mulaem model, the Couture model represents higher nonlinearity with saturation.

Liquid water diffusivity in wood

To estimate the liquid diffusivity, material properties such as the intrinsic and relative permeability, the CSR, and density shoud be given (Eq. 11). However, the intrinsic permeability of wood varies widely among different specimens of the same species as well as between different species. According to Bao et al.,[20] the permeability of wood is not affected by its changing density between and within species. The longitudinal air permeability at moisture content 0.1 ranged between 7.49×10^{-15} m^2 and 1.85×10^{-12} m^2 for softwood, and between 1.80×10^{-15} m^2 and 1.33×10^{-11} m^2 for hardwood.

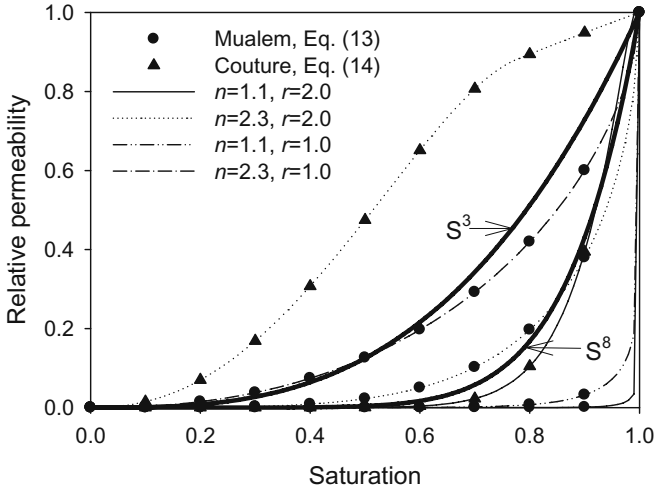

Fig. 2. Comparison of estimated relative permeability of wood by the Mualem and Couture models ($p = 0.5$, $q = 1$). S^3 and S^8 curves refer to Eq. 12

To compare the liquid diffusivity of wood, Eq. 11 can be rearranged as

$$\frac{D_w}{K_w} = -\frac{\rho_w}{\rho_0} \frac{k_{rw}}{\mu_w} \frac{\partial P_c}{\partial S} \frac{\partial S}{\partial m} \tag{15}$$

For the VG model, the gradient of capillary pressure with respect to saturation is expressed as

$$\frac{\partial P_c}{\partial S} = -\frac{\left(S^{-1/m} - 1\right)^{(1-n)/n} S^{-(1+m)/m}}{mn\alpha} \tag{16}$$

Similary for the Durner model,

$$\frac{dS}{dP_c} = \sum_{i=1}^{k} -w_i m_i n_i (\alpha_i P_c)^n \left[1 + (\alpha_i P_c)^n\right]^{-(m_i+1)} \Big/ P_c \tag{17}$$

The maximum possible moisture content of wood is predicted theoretically if the cell cavities remain constant in size during moisture sorption and m_{FSP} is known.

$$m_{max} = m_{FSP} + \frac{\phi}{G_0} \tag{18}$$

where the fiber saturation point of wood m_{FSP} is usually assumed to be 0.3, ϕ is porosity, and G_0 is dry specific gravity.

The porosity of wood may be calculated from the wood and cell wall density using Eq. 4, assuming that the density of bound water is equal to the water density, the oven-dry cell wall density is 1540 kg/m^3, and the pore volume remains constant with the moisture changes.

$$\phi = 1 - \frac{\rho_0}{1540} = 1 - \frac{1000 \times G_0}{1540} \tag{19}$$

However, it is difficult to measure the dry volume because the moisture content can change during measuring. Therefore, the dry specific gravity can be obtained using the moist specific gravity.

$$G_0 = \frac{G_m}{1 - mG_m} \tag{20}$$

where G_m is the specific gravity of wood based on dry weight and moist volume at the given moisture content. The air-dry specific gravity at moisture content 0.12 and green moisture content of heartwood and sapwood are given in Table 7.

Figure 3 shows the estimated D_w/K_w for Eq. 15. There is high variation between wood species. Aspen shows an inflection point around saturation 0.6 due to bimodal pore distributions. D_w/K_w of softwood is higher than that of hardwood in most cases. The liquid diffusivities of red pine and cottonwood sapwood were the highest and Douglas fir and yellow poplar showed the lowest values for softwood and hardwood, respectively. For western hemlock, the average liquid diffusivity for desorption was about 7.7 times higher than that for absorption.

There was no significant difference in D_w/K_w between sapwood and heartwood in the case of American elm. For cottonwood, D_w/K_w for sapwood was higher than for heartwood. For baldcypress, however, D_w/K_w for sapwood was lower than for heartwood.

Table 7. Physical properties of wood species

Species	Wood handbook		Dry density (kg/m^3)	Porosity	Maximum MC	*dS/dm*
	Air-dry specific gravity	Green MC (heart/sap)				
Aspen	0.39	0.95/1.13	409	0.73	2.09	0.56
Red pine	0.46	0.32/1.34	487	0.68	1.70	0.71
Western hemlock	0.45	0.85/1.70	476	0.69	1.75	0.69
American elm	0.50	0.95/0.92	532	0.65	1.53	0.81
Baldcypress	0.46	1.21/1.71	487	0.68	1.70	0.71
Cottonwood	0.35	1.62//1.46	365	0.76	2.39	0.48
Sweetgum	0.52	0.79/1.37	555	0.64	1.45	0.87
Yellow poplar	0.42	0.83/1.06	442	0.71	1.91	0.62
Douglas fir	0.48	0.37/1.15	509	0.67	1.61	0.76

Data from Forest Products Laboratory[29]
MC, Moisture content

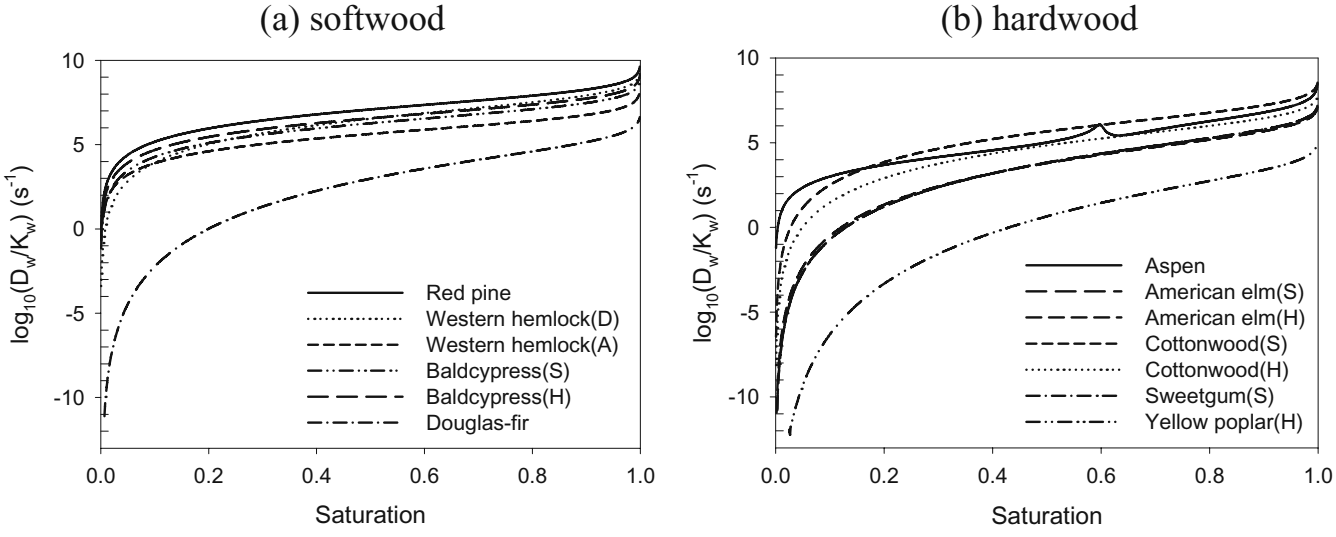

Fig. 3a,b. Estimated liquid diffusivity of wood by the van Genuchten and Durner models ($p = 0.5$, $q = 1$, $r = 2$). *D*, Desorption; *A*, absorption; *S*, sapwood; *H*, heartwood

Conclusions

Assuming that the liquid water transport in wood can be described by Darcy's law, knowledge of the capillary pressure–saturation relation or the capillary pressure–moisture relation, and intrinsic and relative permeabilities is required to simulate the moisture transport model. Investigating the experimental data of wood available in the literature, most species have unimodal pore distributions except for aspen, which has a bimodal pore distribution. The van Genuchten model represented the capillary pressure–water relation better than the Brooks-Corey model. Durner's bimodal model was found to be the most appropriate for the capillary pressure–saturation relation for aspen. For less fitted cases such as Douglas fir with unimodal pore distribution, Durner's bimodal model gave better fitting results than the van Genuchten model. The relative permeability was calculated by using Mualem's model, and was compared with the value obtained from the Couture model. From the results, the liquid water diffusivity divided by intrinsic permeability of wood can be estimated as a function of saturation or moisture content. This approach may be promising for adopting the liquid water diffusivity for numerical simulation of drying and sorption and to minimizing experimentation required for measurement of liquid transport coefficients. In the future, more studies are required on the effects of physicochemical properties of wood on liquid transport parameters because there may be considerable variation within and between trees.

Acknowledgments This work was supported by a Korea Research Foundation Grant funded by the Korean Government (MOEHRD) (The Regional Research Universities Program/Biohousing Research Institute) and the Brain Korea 21 Program funded by the Ministry of Education, Republic of Korea.

References

1. Moyne C, Perre P (1991) Process related to drying: part I – theoretical model. Drying Technol 9:1135–1152
2. Perre P, Moser M, Martin M (1993) Advances in transport phenomena during convective drying with superheated steam and moist air. Int J Heat Mass Transfer 36:2725–2746

3. Couture F, Jomma W, Puiggali JR (1996) Relative permeability relations: a key factor for drying. Transport Porous Med 23:303–335
4. Spolek GA, Plumb OA (1981) Capillary pressure in softwoods. Wood Sci Technol 15:189–199
5. Kang W, Chung WY, Eom CD, Yeo HM (2008) Some considerations in heterogeneous nonisothermal transport models for wood: numerical study. J Wood Sci 54:267–277
6. Kang W, Kang CW, Chung WY, Eom CD, Yeo H (2008) The effect of openings on combined bound water and water vapor diffusion in wood. J Wood Sci 54: 343–348
7. Cloutier A, Fortin Y (1993) A model of moisture movement in wood based on water potential and the determination of the effective water conductivity. Wood Sci Technol 27:95–114
8. Descamps F (1996) Continuum and discrete modeling of isothermal water and air flow in porous media. Ph.D. dissertation, Catholic University of Leuven, Leuven
9. Cloutier A, Fortin Y (1991) Moisture content–water potential relationship of wood from saturated to dry conditions. Wood Sci Technol 25:263–280
10. Fortin Y (1979) Moisture content–matric potential relationship and water flow properties of wood and high moisture contents. Ph.D. dissertation, University of British Columbia, Vancouver
11. Roels S, Elsen J, Carmeliet J, Hens H (2001) Characterisation of pore structure by combining mercury porosimetry and micrography. Mater Struct 34:76–82
12. Brooks RH, Corey AT (1965) Hydraulic properties of porous media. Hydrol Pap 3:1–27
13. Bonneau P, Puiggali JR (1993) Influence of heartwood–sapwood proportions on the drying kinetics of a board. Wood Sci Technol 28:67–85
14. Perre P, Turner I (2001) Determination of the material property variations across the growth ring of softwood for use in a heterogeneous drying model. Part 1. Capillary pressure, tracheid model and absolute permeability. Holzforschung 55:318–323
15. Perre P, Moyne C (1991) Process related to drying: part II – use of the same model to solve transport both in saturated and unsaturated porous media. Drying Technol 9:1153–1179
16. Pang S (1997) Relationship between a diffusion model and a transport model for softwood drying. Wood Fiber Sci 29:58–67
17. Perre P, Turner IW (1999) A 3-D version of TransPore: a comprehensive heat and moisture transport computational model for simulating the drying of porous media. Int J Heat Moisture Transport 42:4501–4521
18. Tremblay C, Cloutier A, Fortin Y (1996) Moisture content–water potential relationship of red pine sapwood above the fiber saturation point and determination of the effective pore size distribution. Wood Sci Technol 30:361–371
19. Choong ET, Tesoro FO (1989) Relationship of capillary pressure and water saturation in wood. Wood Sci Technol 23:139–150
20. Bao F, Lu J, Avramidis S (1999) On the permeability of main wood species in China. Holzforschung 55:350–354
21. van Genuchten MT (1980) A closed-form equation for predicting the hydraulic conductivity of unsaturated soils. Soil Sci Soc Am J 44:892–898
22. Durner W (1994) Hydraulic conductivity estimation for soils with heterogeneous pore structure. Water Resour Res 30:211–223
23. Tesoro FO, Choong ET, Kimbler OK (1974) Relative permeability and the gross pore structure of wood. Wood Fiber 6:226–236
24. Priesack E, Durner W (2006) Closed-form expression for the multi-modal unsaturated conductivity function. Vadose Zone J 5:121–124
25. Koponen H (1987) Moisture diffusion coefficients of wood. In: Mujumdar AS (ed) Drying 87. Hemisphere, New York
26. Kumaran MK (1999) Moisture diffusivity of building materials from water absorption measurements. J Thermal Env Build Sci 22:349–355
27. Cameliet J, Hens H, Roels S (2004) Determination of the liquid water diffusivity from transient moisture transport experiments. J Thermal Env Build Sci 27:277–305
28. Mualem Y (1986) A new model for predicting the hydraulic conductivity of unsaturated porous media. Water Resour Res 12: 513–522
29. Forest Products Laboratory (1999) Wood handbook – wood as an engineering material. Gen Tech Rep FPL-GTR-113. United States Department of Agriculture